



HepG2 spheroids as a biosensor-like cell-based system for (geno) toxicity assessment

Martina Štampar^{a,b}, Sonja Žabkar^a, Metka Filipič^a, Bojana Žegura^{a,*}

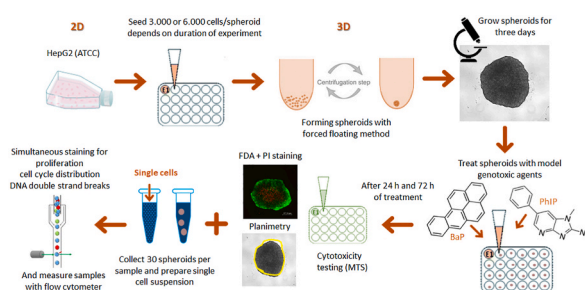
^a Department of Genetic Toxicology and Cancer Biology, National Institute of Biology, Ljubljana, Slovenia

^b Jozef Stefan International Postgraduate School, Ljubljana, Slovenia

HIGHLIGHTS

- HepG2 spheroids can be used as a biosensor-like system for genotoxicity evaluation.
- Flow cytometry allows simultaneous detection of multiple endpoints in the same cell.
- HepG2 spheroids in combination with flow cytometry enable high-content analysis.

GRAPHICAL ABSTRACT



ARTICLE INFO

Handling Editor: Frederik-Jan van Schooten

Keywords:

In vitro 3D cell model
HepG2
Flow cytometry
Cell cycle
Proliferation
DNA strand Breaks

ABSTRACT

3D spheroids developed from HepG2 cells were used as a biosensor-like system for the detection of (geno)toxic effects induced by chemicals. Benzo(a)pyrene (BaP) and amino-1-methyl-6-phenylimidazo[4,5-b]pyridine (PhIP) with well-known mechanisms of action were used for system validation. HepG2 spheroids grown for 3 days were exposed to BaP and PhIP for 24 and 72 h. The growth and viability of spheroids were monitored by planimetry and Live/Dead staining of cells. Multi-parametric flow cytometric analysis was applied for simultaneous detection of specific end-effects including cell cycle analysis (Hoechst staining), cell proliferation (KI67 marker), and DNA double-strand breaks (γ H2AX) induced by genotoxic compounds. Depending on the exposure concentration/time, BaP reduced spheroid growth, affected cell proliferation by arresting cells in S and G2 phase and induced DNA double-strand breaks (DSB). Simultaneous staining of γ H2AX formation and cell cycle analysis revealed that after BaP (10 μ M; 24 h) exposure 60% of cells in G0/G1 phase had DNA DSB, while after 72 h only 20% of cells contained DSB indicating efficient repair of DNA lesions. PhIP did not influence the spheroid size whereas accumulation of cells in the G2 phase occurred after both treatment times. The evaluation of DNA damage revealed that at 200 μ M PhIP 50% of cells in G0/G1 phase had DNA DSB, which after 72-h exposure dropped to 40%, showing lower repair capacity of PhIP-induced DSB compared to BaP-induced. The developed approach using simultaneous detection of several parameters provides mechanistic data and thus contributes to more reliable genotoxicity assessment of chemicals as a high-content screening tool.

* Corresponding author. National Institute of Biology, Department for Genetic Toxicology and Cancer Biology, Vecna pot 111, 1000, Ljubljana, Slovenia.

E-mail addresses: martina.stampar@nib.si (M. Štampar), sonja.zabkar@nib.si (S. Žabkar), metka.filipic@nib.si (M. Filipič), bojana.zegura@nib.si (B. Žegura).

<https://doi.org/10.1016/j.chemosphere.2021.132805>

Received 5 August 2021; Received in revised form 19 October 2021; Accepted 4 November 2021

Available online 9 November 2021

0045-6535/© 2021 The Authors.

Published by Elsevier Ltd.

This is an open access article under the CC BY-NC-ND license

(<http://creativecommons.org/licenses/by-nc-nd/4.0/>).

1. Introduction

Increased development of new chemicals and consumer products, such as drugs, cosmetics, food and feed additives and similar, which are widely used in our everyday life raises concern about the possible adverse effects on human health due to genotoxicity (Corvi and Madia, 2017). Data on the genotoxicity of chemicals that are obligatory for the registration and authorization of chemicals and products are obtained using a battery of short-term genotoxicity tests with bacteria and rodent or human cell lines (Mahadevan et al., 2011). Positive results need to be confirmed in animal models, which are many times unnecessary due to a relatively high proportion of misleading results obtained with *in vitro* test systems. Moreover, currently used animal models, mostly rats and mice, have a weak correlation with humans and thus fail to predict the human outcome, are costly, and are associated with ethical issues (Kirkland et al., 2005). One of the key reasons contributing to the relatively high proportion of false-positive *in vitro* results is the inadequate representation of enzymes involved in the metabolism of xenobiotic compounds in cell lines used for routine genotoxicity evaluation (Kirkland et al., 2007). Recently, the Workshop on Genotoxicity Testing (IWGT) recommended focusing on the development of alternative *in vitro* 3D systems with enhanced liver-like functions to provide cost-effective and reliable tools for the safety assessment of chemicals that will enable high-throughput screening (Pfuhrer et al., 2020) and will follow the “3R” principles (Reduce, Refine and Replace) related to the use of animals for research purposes (Corvi et al., 2013).

Primary human hepatocytes are still considered as a golden standard *in vitro* hepatic experimental model in drug development and toxicity testing (LeCluyse, 2001); however, they rapidly dedifferentiate resulting in the loss of their hepatic phenotype and functionality. Besides, they have limited availability, inter-donor variability, and relatively high cost, which makes them an inappropriate model for routine *in vitro* genotoxicity testing (den Braver-Sewradj et al., 2016; Gomez-Lechon et al., 2004). Therefore, considerable efforts are being dedicated to developing reliable and physiologically relevant, human-derived *in vitro* cell models that will give predictive results for human exposures to genotoxic chemicals and will enable efficient screening. As a result, several models based on hepatocellular carcinoma derived cell lines such as HepG2 (Knasmüller et al., 2004), Huh6 (Waldherr et al., 2018) and HepaRG (Mandon et al., 2019) have been developed. Traditionally these cells are grown in monolayer cultures and it has been demonstrated that under such conditions they do not reflect the physiological properties of tissues and are not appropriate for the prediction of *in vivo* behaviour (Edmondson et al., 2014). The cells grown under the 3D arrangement (i.e. spheroids) are surrounded by the natural extra-cellular matrix (ECM), which promotes tissue-specific architecture, direct cell-cell and cell-extracellular matrix interactions, and thus provides *in vivo*-like environment (Fey and Wrzesinski, 2012; Wrzesinski et al., 2021; Wrzesinski and Fey, 2013). Moreover, the spheroids enable prolonged exposures due to their increased stability as they retain high cell viability and morphology over several weeks (Bell et al., 2016; Bokhari et al., 2007; Eilenberger et al., 2019; Hughes, 2008; Pfuhrer et al., 2020; Shah et al., 2018; Štampar et al., 2020b; Wrzesinski and Fey, 2015). Due to improved characteristics of 3D cell models over 2D cell cultures, the use of liver spheroids in genetic toxicology has increased markedly in the last years (Conway et al., 2020; Elje et al., 2019, 2020; Fey et al., 2020; Llewellyn et al., 2020; Mandon et al., 2019; Pfuhrer et al., 2020; Shah et al., 2018, 2020; Štampar et al., 2019, 2020b).

The threats of genotoxic compounds necessitate not only a sensitive detection regimen but also the employment of a rapid, broad-spectrum screening tool that can be used for high-throughput detection of genotoxic compounds. In the present study, we developed a testing approach utilizing an *in vitro* 3D cell model combined with detection techniques based on microscopy and flow cytometry. The spheroids developed from a human hepatocellular carcinoma cell line (HepG2) were used for the detection of cytotoxic and genotoxic effects induced by model indirect-

acting genotoxic compounds, polycyclic aromatic hydrocarbon (BaP) and heterocyclic aromatic amine (PhIP), which were used for the functional evaluation of the proposed testing approach. The influence of BaP and PhIP on spheroid growth was monitored with planimetry by light microscopy, while the viability was assessed with fluorescent Live/Dead staining using FDA and PI and detected by confocal microscopy. Further, a flow cytometric approach for simultaneous detection of specific lesions including cell cycle analysis (Hoechst staining), cell proliferation (KI67 antibodies), and DNA double-strand breaks (γ H2AX antibodies) was developed. By applying two genotoxic agents (BaP and PhIP) with well-known mechanisms of action, we investigated whether simultaneous sensing of fluorescent signals within exposed cells corresponding to specific effects (formation of DNA double-strand breaks, cell cycle analysis and cell proliferation) could be suited as a high-content screening approach for the detection of (geno)toxic compounds.

2. Materials and methods

2.1. Chemicals

All used chemical and their information are listed in Appendices – Chemicals.

2.2. Cell culture and the formation of spheroids

The HepG2 cells (HB-8065™) provided by the ATCC-Cell bank, were cultured in MEME media under standard cell culture conditions (at 37 °C, 5% CO₂ atmosphere and 95% humidity) as described by Štampar et al. (2019). The spheroids were prepared by the forced floating method, using a growth medium supplemented with 4% methylcellulose (Štampar et al., 2019). In the study, two initial densities of 3000 and 6000 cells/spheroid were used and grown in the static system for 72 h under standard cell culture conditions.

2.3. Treatment conditions

After 72 h of culturing in the static system, the 200 μ l of growth media was replaced with fresh media (200 μ l) containing benzo(a)pyrene (BaP) or amino-1-methyl-6-phenylimidazo[4,5-b]pyridine (PhIP). The spheroids were exposed to BaP at concentrations 0.1, 1, 10, 20 and 40 μ M for 24 h, and 0.001, 0.01, 0.1, 1, 10 μ M for 72 h; and PhIP at concentrations 50, 100, 150, 200 μ M for 24 h, and 25, 50, 100, 150, 200 μ M for 72 h. In all experiments, solvent (0.2 and 1% DMSO for BaP and PhIP, respectively) and appropriate positive controls (PC) were included. In all experiments, no statistical differences between solvent and vehicle control were detected (see appendices Figures A2-A.6).

2.4. Determination of cytotoxic activity by MTS assay

The viability of spheroids was determined by the tetrazolium-based (MTS) assay after 24 and 72 h of exposure as described previously (Štampar et al., 2019). The absorbance was measured using the spectrofluorimeter (Synergy MX, BioTek, USA) at 490 nm. The experiments were performed in three independent biological replicates and each time five spheroids per treatment were measured. Etoposide (1.7 μ M) was used as a PC. The difference between treated groups and the solvent control was analysed by the One-way ANOVA with the posthoc multiple comparisons Dunnett's test using GraphPad Prism V6 (GraphPad Software, California USA). * $p < 0.05$ was considered statistically significant.

2.5. Monitoring of spheroid's growth

The surface area of at least ten spheroids with the initial density of 6000 cells/spheroid and 3000 cells/spheroid was monitored after 72 h of culturing and additional 24 h (altogether 96 h old spheroids), and 72 h of treatment (altogether 144 h old spheroids), respectively, with BaP

and PhIP at applied concentrations. The surface area (mm^2) of each spheroid was determined by planimetry using the NIS elements software 4.13 V at 100x magnification (Nikon Instruments, Melville, NY, USA) connected to the Ti Eclipse inverted microscope (Nikon, Japan). Growth monitoring was conducted in three independent biological replicates.

2.6. Determination of the ratio of live/dead cells in the spheroids by confocal Z-stack imaging

Three live spheroids were stained and monitored after 24 and 72 h exposure to BaP (20 and 10 μM , respectively) and PhIP (200 μM) for each condition (6000 and 3000 cells/spheroid, respectively) (Štampar et al., 2020a). The Leica confocal software connected to the confocal microscope Leica SP8 TCS at 100x magnification was used to capture the Z-stack images of single spheroids. Etoposide (1.7 μM) was used as a PC. Along the entire spheroid thickness, the Z-stacks of optical sections were taken using suitable excitation and emission settings for simultaneous dual-channel recordings (PI: 493/636 nm, FDA: 488/530 nm). The Image-Pro 10 software (Media Cybernetics, USA) was used for the image analysis and the quantification of the proportion of dead cells. At least 20 stacks per spheroid were quantified, and the percentage of dead cells in the spheroid was calculated as a ratio between the whole spheroid area and the number of dead cells. Z-stacks of spheroids were presented as a 'maximum intensity projection image' gallery. The analysis provided a numerical value for the area of the spheroid. The difference between treated groups and solvent control was analysed by Student t-test using GraphPad Prism V6 Software. * $p < 0.05$ was considered statistically significant.

2.7. Simultaneous measurement of the cell cycle, cell proliferation and gamma-H2AX positive cells by flow cytometry

The flow cytometric analysis of the cell cycle, cell proliferation, and gamma-H2AX positive cells was performed on the single-cell suspension obtained from a pool of 30 spheroids treated with BaP and PhIP for 24 (initial density 6000 cell/well) and 72 h (initial density 3000 cells/spheroid) of exposure (Štampar et al., 2020a). Fixed cells were washed in cold PBS and labelled with anti-H2AX pS139-APC and anti-KI67-FITC (50-fold diluted antibodies in 1% BSA), washed with PBS, and subsequently stained with Hoechst 33258 dye (diluted in 0.1% Triton X-100 1:500) as described by Hercog et al. (2019) and Štampar et al. (2020a). The flow cytometric measurements were conducted on a MACSQuant Analyzer 10 (Miltenyi Biotech, Germany). Hoechst fluorescence was detected in the V1 (450/500 nm) channel; FITC fluorescence was detected in the B1 (525/500 nm) channel and APC fluorescence was detected in the R1 (655–730 nm) channel. Rea-FITC and rea-APC controls (Miltenyi Biotech, Germany) excluded the unspecific binding of antibodies. The experiment was repeated four times independently, where 20000 single cells per experimental point were recorded. The obtained data were analysed and graphically presented in the FlowJo software V10 (Becton Dickinson, New Jersey USA).

2.8. Statistical analysis of the results obtained by flow cytometry

The analysis of the frequency distributions of cells in the cell cycle (the percentage of cells in the G0/G1, S, and G2 phase) was conducted by the multinomial logistic regression, and further post estimation tests in Stata 15 (StataCorp LLC, USA). Multinomial logistic regression is an advanced classification technique that allows us to predict the probabilities of different possible outcomes (G0/G1, S, and G2) given a set of independent variables. Specifically, it enabled us to assess the effect of different concentrations of model genotoxic compounds on the cell cycle distribution. Additional pairwise comparisons of the predicted probabilities were conducted using the Bonferroni correction to account for the multiple comparisons, which allowed us to identify the differences between each treatment. The difference in the amount of KI67 positive

cells in exposed and control cell populations was tested by the one-way ANOVA with Dunnett's multiple comparison test, using GraphPad V6 Software. The proportion of yH2AX positive cells in each phase (G0/G1, S, G2) relative to all cells in the cell cycle was determined in FlowJo software V10 (Becton Dickinson, New Jersey USA) and the statistical significance was tested by the one-way ANOVA with Dunnett's multiple comparison test, using GraphPad V6 Software. The statistically significant difference in the APC fluorescence between treated and control groups was tested using exported. csv values in the R software with the Mixed Effects Models (nlme) package by REML (Pinheiro et al., 2007). Furthermore, additional marginal effects were calculated in Stata 15 (StataCorp LLC, USA) for an easier assessment of the results.

3. Results and discussion

There is an ever-increasing need for the development of fast, reliable and physiologically relevant *in vitro* models for the safety assessment of various chemicals, and, more recently, for the screening of pharmaceuticals, food and agricultural products, and environmental samples, which all emerged as a major concern due to significant impact on human health. Currently, there is an ongoing trend to develop standardized and robust *in vitro* hepatic 3D cell models, which closely resemble an *in vivo* microenvironment and can be used for toxicity assessment (Elje et al., 2020; Fey et al., 2020; Guo et al., 2019; Hurrell et al., 2019; Mandon et al., 2019; Pfuhrer et al., 2020).

In the present study, we developed a biosensor-like cell-based approach with HepG2 spheroids for the detection of cytotoxic and genotoxic activity of chemicals with simultaneous measurement of three end-points: influence on cell cycle distribution, cell proliferation and induction of DNA damage. Two model indirect-acting genotoxic compounds, benzo(a)pyrene (BaP) and 2-Amino-1-methyl-6-phenylimidazo [4,5-b]pyridine (PhIP) were selected for the validation of the system. For the formation of spheroids we used the forced floating method and for culturing the static system was used, which enables culturing up to 14-days (Štampar et al., 2020a).

3.1. The impact of BaP and PhIP on growth and viability of HepG2 spheroids

The growth of spheroids after the exposure to graded concentrations of BaP and PhIP for 24 h and 72 h was monitored by measuring and quantifying the average spheroid area by planimetry (Table A. 1). The results showed that BaP at 20 μM and 10 μM after 24 and 72 h exposure, respectively, statistically significantly decreased the spheroids' average surface area compared to solvent control spheroids (Fig. 1 A and 1 B). PhIP on the other hand, after 24 h did not significantly influence the average surface area of spheroids (Fig. 1C and A. 1C), while after prolonged (72 h) exposure a trend of reduced spheroid average surface area was observed compared to solvent control but was not statistically important (Fig. 1 D and A. 1 D). The positive control (ET at 1.7 μM) significantly reduced the average surface area of spheroids after 72 h exposure. Similar results were reported for 21-day old HepG2/C3A spheroids grown in bioreactors under dynamic conditions that were exposed for 24 and 96 h to BaP (40 and 4 μM , respectively) and PhIP (200 and 400, respectively) (Štampar et al., 2020b).

The impact of BaP and PhIP on spheroid's cell viability was measured with the tetrazolium-based (MTS) assay (Fig. 2A–D) and with differential staining of the whole spheroid with FDA and PI (Fig. 2 (E–H)). Spheroids with the initial density of 6000 and 3000 cells/spheroid grown for 3 days were exposed to graded concentrations of each compound. The MTS assay results revealed that BaP did not affect the viability of cells at the applied conditions (Fig. 2A and B), which is in line with the results reported by (Štampar et al., 2019). In 21-day old HepG2/C3A spheroids grown in dynamic bioreactors, BaP at 40 μM and 4 μM after 24 and 96 h exposure, respectively, reduced cell viability measured by the ATP content (Štampar et al., 2020b), while in 10-day

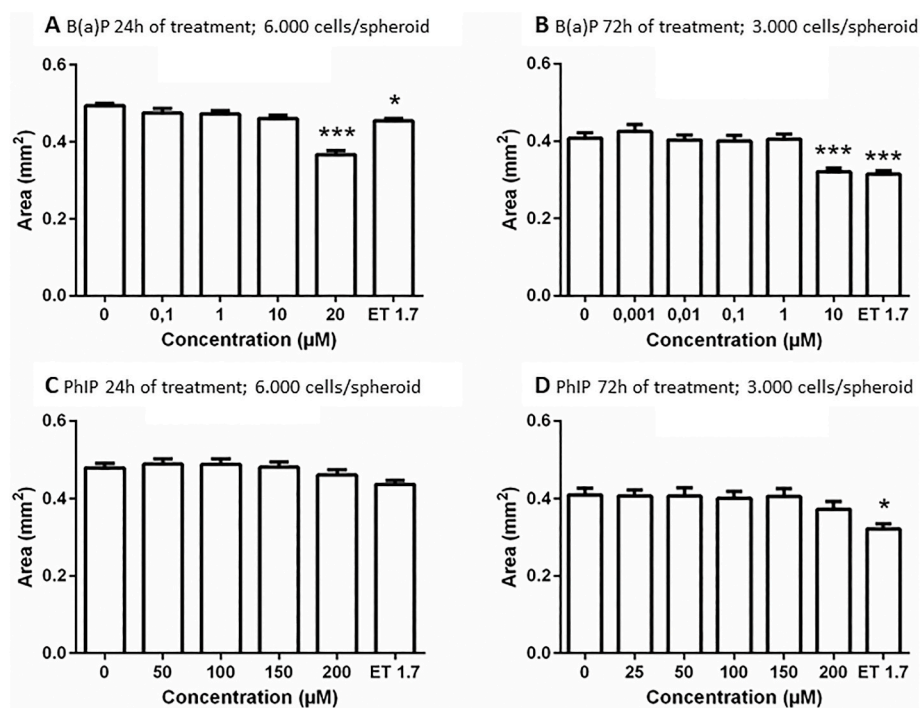


Fig. 1. Planimetry of three-day-old spheroids monitored after (A–C) short-term (24 h) and (B–D) long-term (72 h) treatment with graded concentrations of BaP (A–B) and PhIP (C–D). The growth of spheroids was monitored at 10X magnification (Nikon Instruments) with the Ti Eclipse inverted microscope (Nikon). ET (1.7 μM etoposide) was the positive control. The results are presented as the mean ± SD (N = 10). The statistical analysis was conducted in Graph Pad Prism 6, by the one-way ANOVA using the Dunnett's multiple comparisons tests, *p < 0.05, **p < 0.01, ***p < 0.001.

old HepaRG spheroids 24 h exposure to B(a)P at concentrations of up to 20 μM no effect on cell viability was reported (Mandon et al., 2019). On the other hand, we showed that PhIP at 400 μM after 72 h exposure significantly decreased cell viability in HepG2 spheroids by approximately 24% (Fig. 2 D). Previously, a slight though significant decrease in cell viability upon 24 h exposure of HepG2 spheroids to PhIP (200 μM) (Štampar et al., 2019) and 21-day old HepG2/C3A spheroids to PhIP (400 μM) (Štampar et al., 2020b) was reported. In monolayer cultures, significant effects of PhIP on HepG2 cell survival were also shown; however, at lower concentrations (Pezdiric et al., 2013; Štampar et al., 2019). A positive control, etoposide (1.7 μM) after 72 h exposure significantly reduced cell viability by approximately 20% (Fig. 1 B and D).

Further, Live/Dead staining was conducted on whole spheroids treated with the highest BaP (24 h: 20 μM and 72 h: 10 μM) (Fig. 2 E, G) and PhIP (24 h: 200 μM and 72 h: 200 μM) concentration (Fig. 2 F, H)). After quantification of fluorescent images, where red fluorescently stained nuclei are used to estimate dead cells and green fluorescently stained cells present the total number of live cells, an increased percentage of dead cells was determined at 20 μM BaP after 24-h exposure, but was not significantly different from the control spheroids, while significant increase compared to control was determined after 72 h exposure to 10 μM BaP. No increased red fluorescence corresponding to dead cells was notified after 24-h exposure to PhIP, while after 72 h exposure to 200 μM PhIP the percentage of dead cells increased significantly. The positive control, etoposide, significantly increased the percentage of dead cells (approximately 45%) after 72 h. The image-based analysis allows the visualization of spheroids along the Z-axis, thus enabling the observation of cells located inside and not only on the surface of spheroids. This enables to differentiate the occurrence of dead cells within the spheroid.

3.2. The impact of BaP and PhIP on cell cycle, cell proliferation and DNA damage

The impact of the exposure to BaP and PhIP at two different time points (24 and 72 h) on the cell cycle, cell proliferation, and DNA double-strand break formation was studied by simultaneous

measurement of fluorescent signals of the dye Hoechst 33258 for cell cycle analysis and anti-bodies, FITC coinciding to the proliferation marker KI67, and APC coinciding to DNA double-strand breaks detected by flow cytometry. This approach enables the study of several endpoints simultaneously in the same cell within the cell population and can be used as a high-content screening tool for the determination of (geno)toxic effects induced by various chemicals and complex mixtures (Patra et al., 2016). The single-cell suspension from HepG2 spheroids was obtained by mechanical degradation and enzymatic digestion (HS et al., 2021; Štampar et al., 2019). The viability of cells determined by Trypan blue staining accounted for ≥80% of viable cells (data not shown).

The cell cycle of proliferating eukaryotic cells consists of four phases, namely G1, S, G2, and M and is regulated at several checkpoints, with the most important being G1/S and G2/M, where crucial decisions on DNA replication and the completion of the cell division are made (Bartek and Lukas, 2001). In the case of DNA damage, the cell cycle is arrested until the damage is repaired, which causes the accumulation of cells in one of the checkpoints. If DNA damage cannot be repaired, the cells undergo apoptosis (Andrew Murray and Tim Hunt, 1994) or mutations can occur (Lodish et al., 2000). In HepG2 spheroids after 24-h exposure, BaP arrested cells in the S phase in a concentration-dependent manner with concomitant reduction of the cell number in the G1 phase. At 20 μM BaP also reduced the number of cells in the G2/M phase (Fig. 3 A). After prolonged exposure to 10 μM BaP, a significant decrease of cells in G1 and a concomitant significant increase of cells in the G2/M phase were noticed (Fig. 3 C). This is in line with previous reports showing that DNA damage induced by BaP activates the S-phase and G2/M checkpoints in human cell lines (e.g. HepG2, MCF7), allowing the majority of cells to survive (Caino et al., 2007; Hockley et al., 2006; Jeffy et al., 2000; Stellas et al., 2014). Consequently, a part of cells re-enters the cell cycle while carrying significant amounts of residual damage, which persists even when the cells complete the first and enter the second cycle, leading to a new round of checkpoint kinase 1 (Chk1) activation. Activation of Chk1 holds the cell in the G2 phase until ready to enter the mitotic phase. This delay allows time for DNA damage to be repaired or the initiation of cell death if DNA damage is irreparable. However, such repeated Chk1 activations are leading to the failure of the cells to divide

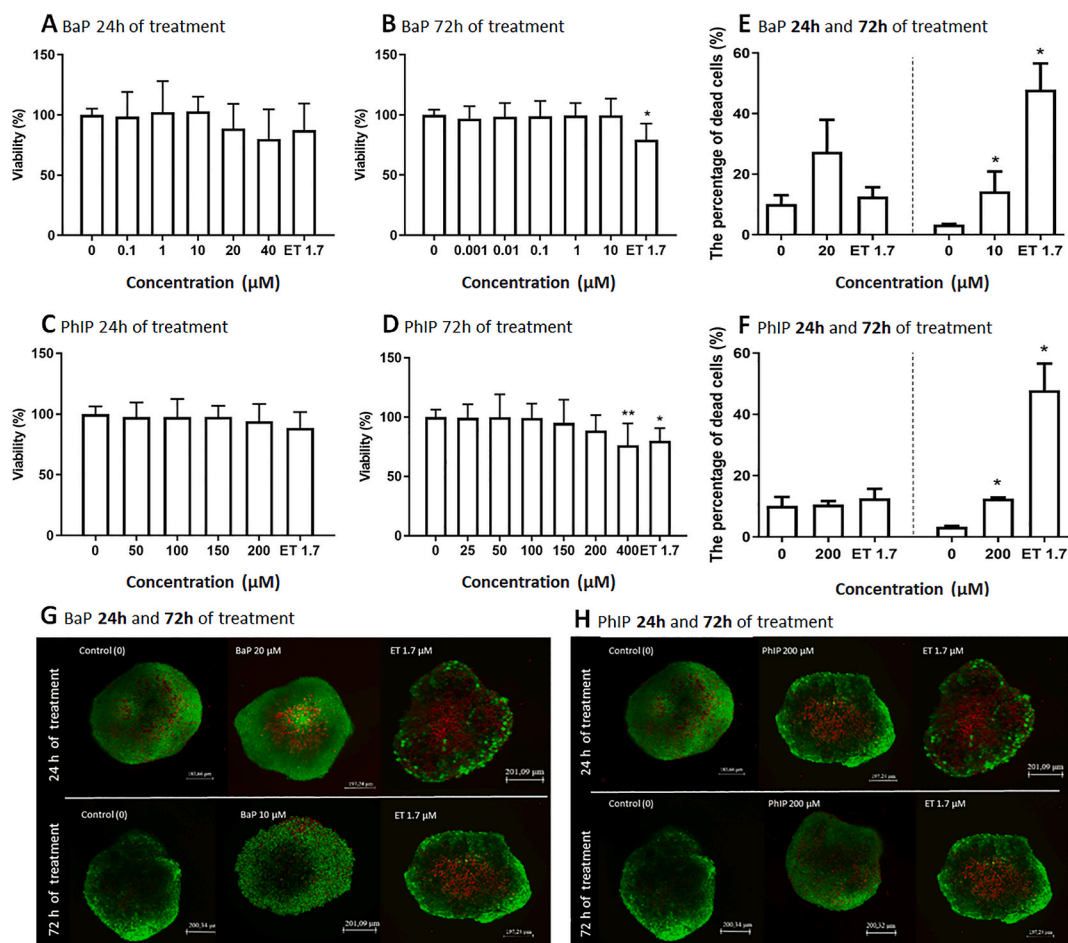


Fig. 2. Cell viability (A–D), the quantification of Z-stacks (E–F) and the images of Live/Dead staining (G–H) of HepG2 spheroids after 24 and 72 h of exposure to graded concentrations of BaP (A, B, E and G) and PhIP (C, D, F and H) determined with the MTS assay, and Live/Dead staining. For viability, the results were normalized to the solvent control (0.2% DMSO for BaP and 1% DMSO for PhIP). The results are given as a mean value of three independent experiments \pm SD. The statistical analysis was performed by the one-way analysis of variance – ANOVA, using Dunnett’s multiple comparisons tests (* $p < 0.05$, ** $p < 0.01$). The live spheroids were stained with FDA (green, live cells) and PI (red, dead cells). The Z-stacks were obtained using a confocal microscope at 100 \times -magnification and a collection of 50 Z-stacks images was presented as a gallery of ‘maximum intensity projection image’. The quantification was conducted with ImagePro 10 software, where at least 20 stacks per spheroid were measured, and the percentage of dead cells in the spheroid was calculated ($n = 3$). The statistical significance was calculated with the Student t-test, with * $p < 0.05$. Etoposide 1.7 μM was considered as a positive control. (For interpretation of the references to colour in this figure legend, the reader is referred to the Web version of this article.)

correctly and increase the frequency of mitotic abnormalities (Löffler et al., 2007; Wilsker et al., 2008). Our results, calculated by a multinomial logistic regression, confirmed that BaP arrested cells in the S and G2/M phase after short and prolonged exposure, respectively (Fig. 3 B, D). However, the effect on the cell cycle was lower compared to monolayer cultures as described by Stellas et al. (2014). This can be ascribed to the difference in physiological attributes (both structural and metabolically) between 3D and 2D cell models (Wrzesinski et al., 2014). Furthermore, the calculated predicted probabilities (see Fig. 3 B, D), showed accumulation of cells in the S phase (by 16.4 percentage points) with a decrease of cells in the G1 and G2 phase (–12.4 and –3.9 percentage points, respectively), upon 24-h exposure to BaP (20 μM), meaning that probably the interruption of DNA synthesis had occurred, which was also reported in other studies (Hockley et al., 2006; Jeffy et al., 2000). The arrest in DNA synthesis probably occurs due to the intra-S checkpoint, which enables the recognition of damaged DNA and repair time, while avoiding the irreversible errors during replication (Hamouchene et al., 2011). After prolonged BaP exposure (10 μM ; 72 h), the predicted probability indicated a significant decrease of cell number in G1 (by –9.0 percentage points) and a concomitant increase of cells in the G2 phase (by 9.9 percentage points), clearly showing the arrest of cells in the G2/M phase of the cell cycle.

In spheroids exposed to PhIP (200 μM) the accumulation of cells in the G2 phase was observed after 24 and 72 h (Fig. 3 E, G). The predicted probability at 24 h exposure for each phase of the cell cycle was minimal, while after prolonged exposure (72 h), the predicted probability of the cells to be in the G1 phase started gradually to decrease in a concentration-dependent manner (Fig. 3 F, H). At the same time, the predicted probability of cells to be in the S and G2 phase increased. The pairwise comparisons of the predicted probabilities, presented in the supplementary Tables A. 2–A. 5, confirmed the effect of BaP on the cell cycle distribution after 24 and 72 h and negligible effect of PhIP after 24 h and stronger effect after 72 h of exposure. In line with our results, is the study on HepG2 monolayer culture, where PhIP at 200 μM induced the accumulation of cells in the S phase and decreased the number of cells in the G0/G1 phase after 24 h exposure (Pezdiric et al., 2013). Furthermore, Zhu et al. (2000) also reported accumulation of human lymphoblastoid TK6 cells in the S phase upon short-term PhIP exposure (20 and 40 h) particularly at higher (5–10 $\mu\text{g}/\text{ml}$ corresponding to 2.3–4.5 μM) concentrations. In HepG2 spheroids, a positive control, etoposide, a DNA topoisomerase inhibitor, clearly arrested the cells in the G2 phase at both exposure times, which complies with its well-known mechanism of action (Bergant Loboda et al., 2020; Hercog et al., 2020).

It is known that cells grown in 3D conformation have reduced

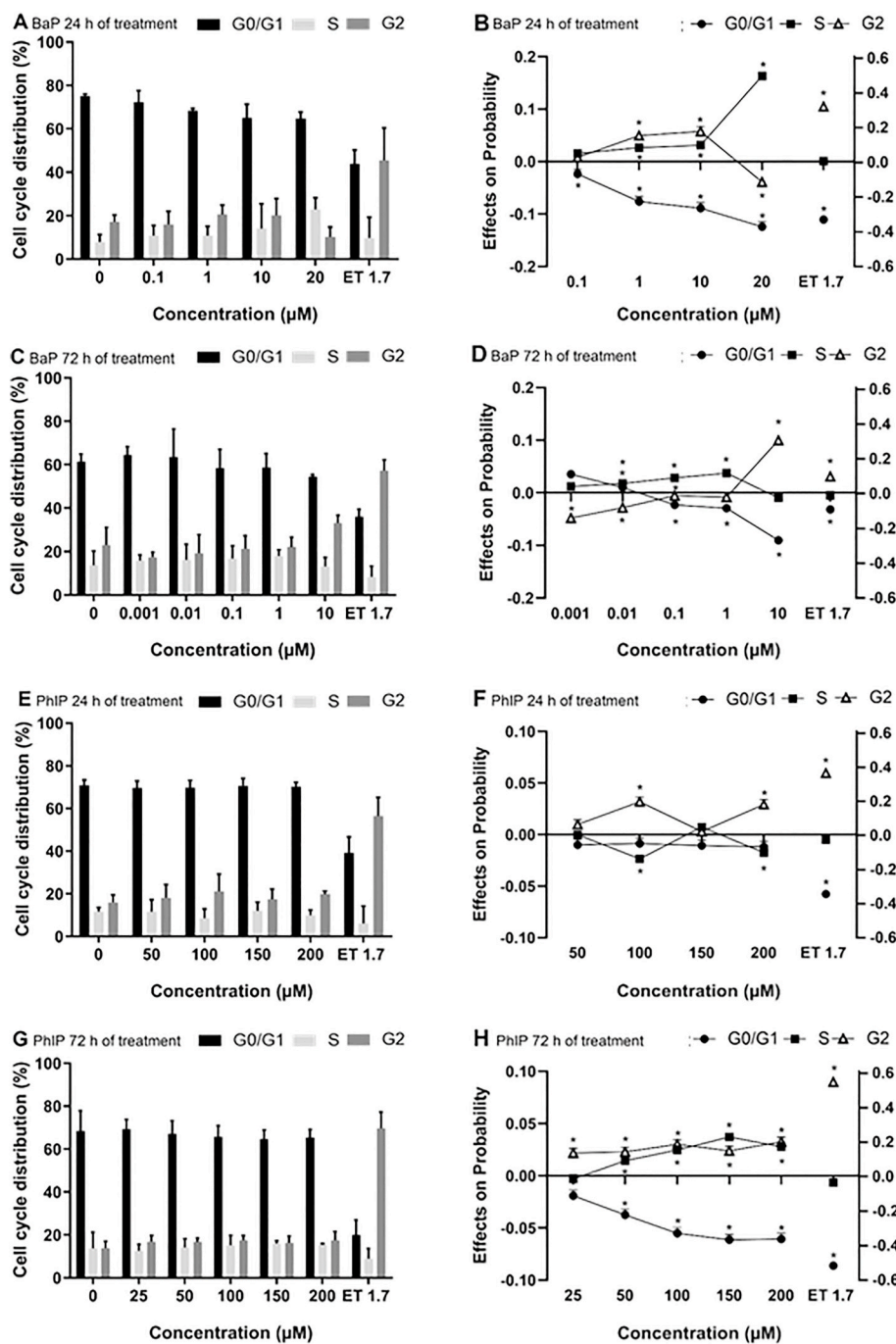


Fig. 3. Distribution of cells across the phases of the cell cycle measured after 24 and 72 h of exposure to BaP (A, C) and PhIP (E, G) and the predicted probabilities of BaP (B, D) and PhIP with 95% CIs (F, H). Etosipide 1.7 μM was considered as a positive control. The cell cycle results are presented as the mean \pm SD (N = 3). The probabilities were calculated in Stata 15 using a multinomial logistic regression * $p < 0.05$. The effects are shown concerning the corresponding solvent control (marked as 0). Statistically significant differences compared to corresponding solvent control are marked with * (* $p < 0.05$).

proliferation (Eilenberger et al., 2019; Štampar et al., 2020a), which leads to self-organization and differentiation of cells in spheroids (Hurrell et al., 2019; Ramaiahgari et al., 2014). Thus, we further studied the effects of BaP and PhIP on the proliferation of the same cell population from the HepG2 spheroids as evaluated for the cell cycle distribution by flow cytometric detection of anti-KI67 antibody through the fluorescent signals of FITC corresponding to the proliferation marker KI67. The Ki-67 protein is an excellent marker for determining the so-called growth fraction of a given cell population (Scholzen and Gerdes, 2000) since it is present in all active phases of the cell cycle (G1, S, G2, and mitosis) and is absent from the resting cells (G0). We notified that $43.2 \pm 4.3\%$ of cells from control spheroids that were for four days in culture (3 days of spheroid formation + additional 24 h) proliferated, while upon 24 h exposure to BaP at 20 μM only $32.1 \pm 7.4\%$ cells

proliferated clearly showing BaP impact on cell proliferation. Further, only $28.1 \pm 5.7\%$ of cells from control spheroids that were for six days in culture (3 days of spheroid formation + additional 72 h) proliferated. BaP at 1 and 10 μM reduced cell proliferation to $19.8 \pm 7.6\%$ and $18.6 \pm 9.9\%$, respectively, (Fig. 4 A, B), indicating BaP influence on HepG2 cell division even after prolonged exposure. On the contrary, PhIP at applied exposures (24 and 72 h) did not significantly affect cell proliferation compared to control (Fig. 4C, D); however, a trend of decreased proliferation was noticed. A decrease of approximately 7.1% of KI67 positive cells compared to the control group was noticed after 24 h exposure to 200 μM PhIP. In spheroids, exposed to etosipide, increased percentage of KI-67 positive cells was measured ($\approx 52\%$), however, this was not due to increased cell proliferation but due to the accumulation of viable cells in G2 phase as shown in the cell cycle analysis (Fig. 3 E, G).

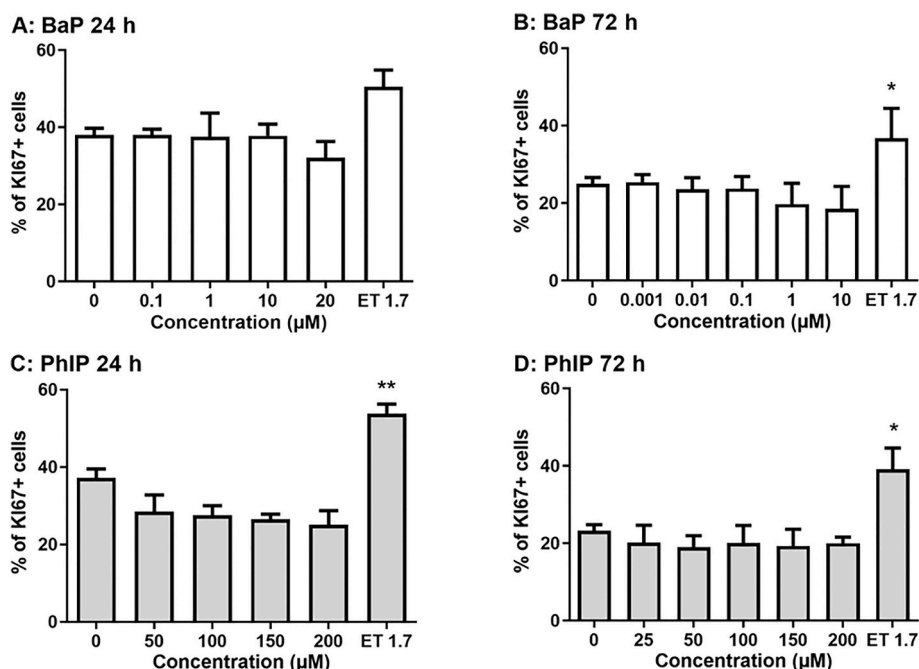


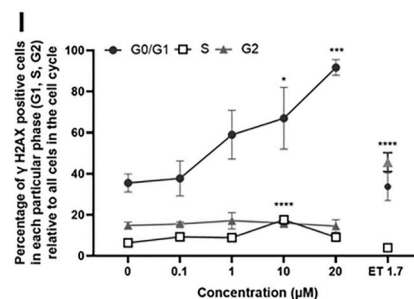
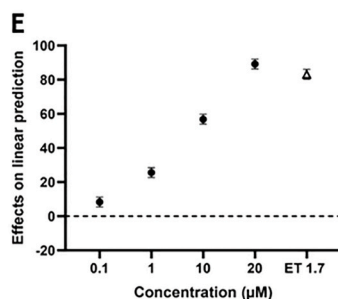
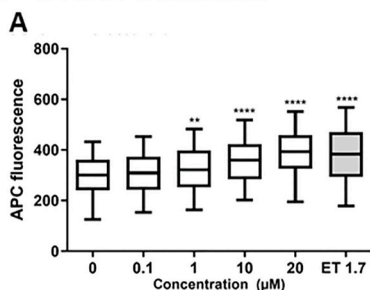
Fig. 4. The percentage of KI67 positive cells (A, C) and the percentage of KI67 positive cells within the G0/G1 phase (B, D) of the cell cycle after 24 and 72 h of exposure to graded concentrations of BaP (A, B) and PhIP (C, D). PC = 1.7 μM etoposide. The results are presented as the mean \pm SD (N = 3). The statistical analysis was conducted in Graph Pad Prism 6, by the two-way ANOVA using the Bonferroni multiple comparisons test, **p < 0.01.

The third end-point measured in the same population of cells isolated from HepG2 spheroids was phosphorylated histone H2AX (γH2AX) that was reported as a promising early and sensitive marker for DNA double-strand breaks (DSB) and DNA adducts (Kopp et al., 2018). The results from our study showed that BaP after 24 and 72 h exposure induced a dose-dependent increase of DNA DSB in HepG2 spheroids, which significantly differed from control $\geq 1 \mu\text{M}$ at both exposure times (Fig. 5 A, B). This was confirmed by the calculated predicted probabilities (Fig. 5E and F), in the amount of DNA DSB between the solvent control and treated samples. Similarly, the induction of DNA DSB by BaP (10 and 30 μM) was also shown in HepG2/C3A spheroids (Coltman et al., 2021). Previously, using the comet assay as a detection method, BaP was shown to induce DNA single-strand breaks in spheroids developed from HepG2 cells at $\geq 10 \mu\text{M}$ (Štampar et al., 2019), HepG2/C3A cells at $\geq 40 \mu\text{M}$ (Coltman et al., 2021; Štampar et al., 2020b) and HepaRG cells at 20 μM (Mandon et al., 2019) after 24 h of exposure. Besides, micronuclei formation upon BaP at 3–8 μM (Shah et al., 2018) was reported in 3D HepG2 hanging drop spheroids (Shah et al., 2018) and the induction was 2-fold higher compared to HepG2 monolayer culture (Shah et al., 2018), revealing that HepG2 spheroids are a very sensitive cell model for detection of genotoxic compounds. When comparing the results of all three assays we can conclude that flow cytometric analysis of γH2AX lesions proved to be the most sensitive marker as it detected DNA damage at the lowest BaP concentration and could be a good choice for screening purposes. Furthermore, the results of the present study clearly showed that cell defence against BaP induced DNA damage was activated in HepG2 cells, which was indicated by the induction of cell-cycle arrest. BaP (20 μM) induced DNA DSB, which was followed by the arrest of cells in the S phase (Figs. 5 A and 4 A). It is known that DNA DSB induce the arrest of cells in the S-phase of DNA synthesis, which occurs via a p53-independent ATM pathway (Kastan et al., 2000). Additionally, we conducted an advanced analysis by combining the results of cell cycle analysis and γH2AX positive cells. The simultaneous staining and measurement of these two endpoints enabled us to accurately determine in which cell phase the cells with DNA DSB were. Further, we calculated the proportion of γH2AX positive cells in each cell cycle phase (G0/G1, S, G2) relative to all cells included in the analysis (Fig. 5 I–L). Clear dose

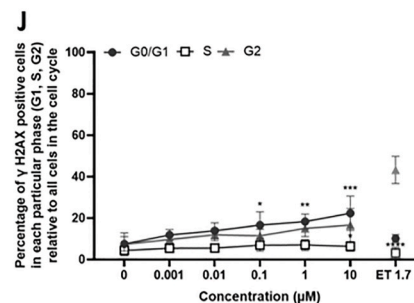
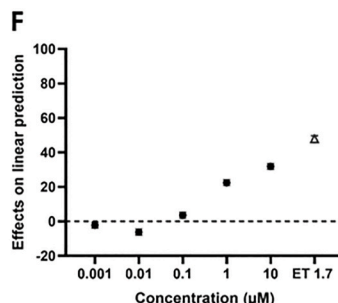
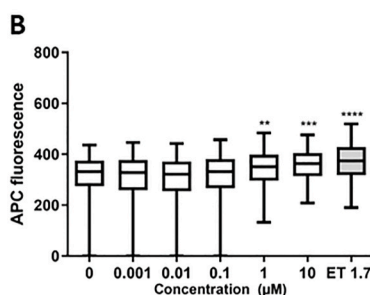
dependent increase in the percentage of cells with DNA DSB in G0/G1 phase after 24 h of exposure to BaP was determined, while after 72 h this percentage was much lower (Fig. 5 I and J). On the contrary, no important differences in the number of cells with DNA DSB were determined for the S and G2 phase when compared to control. Moreover, from the results it can be seen that after 24-h at 10 and 20 μM BaP DNA DSB were detected approximately in 67% and 92% of cells, respectively, which were in G0/G1 phase. After 72 h, DNA DSB were detected in only $\approx 20\%$ of the cells that were exposed to 10 μM BaP. Altogether, this suggests that with time DNA DSB induced by BaP were repaired. Previously, in hepatic spheroids developed from HepG2/C3A cells, a sub-clone of HepG2 cells (Bandelet et al., 2012) that were grown for 21 days in bioreactors and were exposed to BaP for 24 (40 μM) and 96 (4 μM) hours, increased gene expression of *CYP1A1* was reported (Štampar et al., 2020b). Similarly, in HepG2 spheroids grown for three days and exposed to BaP (40 μM) for 24 h the mRNA level of *CYP1A1* and *CYP1A2* (Štampar et al., 2019) encoding the most important phase I enzymes involved in metabolic activation of BaP (Arlt et al., 2008). In the same study, also the genes encoding phase II enzymes (detoxification), namely *UGT1A1* and *SULT1B1* were upregulated (Štampar et al., 2019), suggesting that BaP is metabolized in HepG2 spheroids already within 24 h of exposure.

The second model genotoxic compound, PhIP significantly increased DNA DSB at ≥ 200 and $\geq 25 \mu\text{M}$ after 24 and 72 h exposure, respectively (Fig. 5 C and D), which was confirmed by the linear prediction (Fig. 5 G and H). Previously, PhIP was reported to induce DNA damage after 24 h in HepaRG spheroids at 40 μM (Mandon et al., 2019), HepG2/C3A at 30 μM (Coltman et al., 2021) and HepG2 spheroids at $\geq 50 \mu\text{M}$ (Štampar et al., 2019) determined with the comet assay. Moreover, in 21-day old HepG2/C3A spheroids DNA strand breaks induced by PhIP ($\geq 200 \mu\text{M}$) were determined after 24 h with the comet assay, while after prolonged exposure of 96 h no DNA damage was detected (Štampar et al., 2020b). Besides DNA strand breaks, PhIP ($\geq 3 \mu\text{M}$) induced the formation of micronuclei in HepG2 spheroids as reported by Shah et al. (2018). In the present study, by analyzing the percentage of γH2AX positive cells in each phase of the cell cycle (G0/G1, S, G2) relative to all measured cells in the corresponding group (Fig. 5 K and L), a dose depended increase of

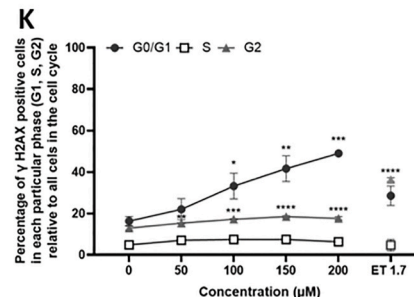
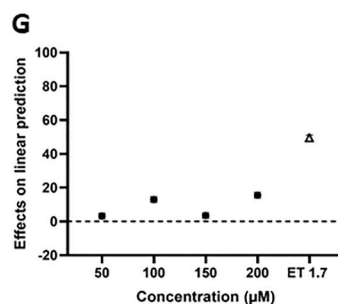
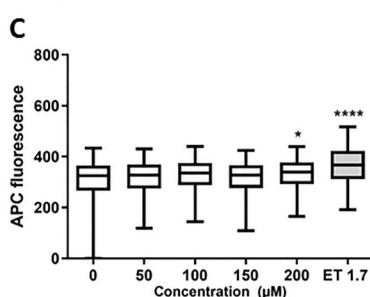
BaP - 24 h of treatment



BaP - 72 h of treatment



PhIP - 24 h of treatment



PhIP - 72 h of treatment

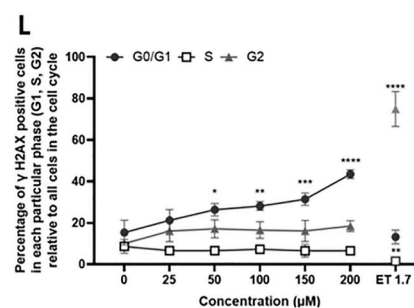
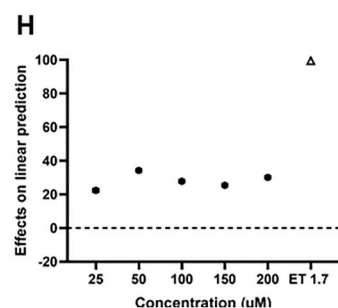
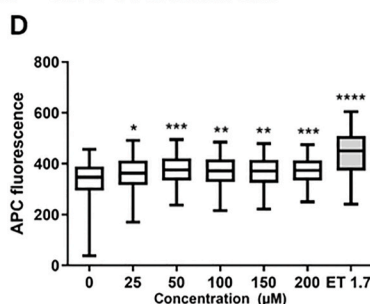


Fig. 5. Relative values of APC fluorescence corresponding to anti- γ H2AX labelled sites (A–D); the predicted probabilities of BaP and PhIP with 95% CIs after 24 (E, G and 72 (F, H) h of exposure to graded concentrations of BaP and PhIP and percentage of γ H2AX positive cells in each cell cycle phase (G0/G1, S and G2) after 24 (I, K) and 72 (J, L) h of exposure. PC = 1.7 μ M etoposide. Significant difference between the treated sample and the solvent control (0) for γ H2AX was tested using the R software with the Mixed Effects Models (nlme) package by REML and is indicated by * $p < 0.05$, ** $p < 0.01$, *** $p < 0.001$ and **** $p < 0.0001$. The effects of probability were calculated in Stata 15 using a multinomial logistic regression * $p < 0.05$. The effects are shown with respect to the solvent control (marked as 0). The results for the percentage of γ H2AX positive cells in each phase (G0/G1, S, G2) relative to all cells in the cell cycle are presented as the mean \pm SD (N = 3). The statistical analysis was conducted in Graph Pad Prism 6, by the one-way ANOVA using the Bonferroni multiple comparisons test, $\alpha = 0.05$.

γ H2AX positive cells was determined in G0/G1 phase of PhIP exposed spheroids after both exposure times. After 24 h exposure to PhIP at 150 and 200 μ M, 42% and 49% of γ H2AX positive cells, respectively, were detected in G0/G1 phase, while after 72 h 31% and 44% of cells with DNA DSB were measured, respectively (Fig. 5 K and L). Similarly, as in the case of BaP also here no important differences in the percentage of γ H2AX positive cells in the S and G2 phase were noticed. Shah et al. (2018) reported that exposure to PhIP can increase activities of CYP1A2

enzyme, and it upregulate the mRNA expression of several phases I and II metabolic enzymes (Stampar et al., 2019, 2020b). Altogether, the literature data and results obtained within the present study indicate that PhIP is metabolized and detoxified in hepatic spheroids and that DNA damage induced by PhIP is repaired as already suggested in the previous study (Stampar et al., 2020b). After 24 h, etoposide-induced DNA DSB in approximately 30% of cells within G0/G1 and G2 phase each (Fig. 4I–L), while after 72 h DNA DSB were detected in more than

70% of cells within the G2 phase, while less than 10% of cells within G0/G1 and S phase were γ H2AX positive.

4. Conclusions

The significant increase of chemicals to which humans can be exposed calls for the development of rapid and reliable research methodologies and approaches to monitor their (geno)toxic activities and possible adverse human health effects. In the last few years, there is an ongoing development of novel 3D cell-based systems, which can provide a better understanding of the processes taking place in living cells and organs. In this context, hepatic spheroids represent an alternative to animal models that can be due to the improved structural, physiological and metabolic properties exploited for broad applications, including (geno)toxicity studies. Furthermore, high-throughput and high-content flow cytometry has developed into a leading technology that supports many applications designed to study the nature of individual cells within homogeneous or mixed cell populations. In the present study, HepG2 spheroids were used as a biosensor-like model for high content toxicity and genotoxicity screening combining confocal microscopy and quantitative image analysis, which allowed us to address biological questions related to the cell viability and growth of spheroids affected by time and genotoxic agents. Further, simultaneous staining of multiple endpoints in the same cell ranging from DNA double-strand breaks (γ H2Ax), proliferation marker (KI-67) and cell cycle using specific antibodies and fluorescent signalling combined with flow cytometry enabled us to track the cells with damaged DNA within the cell cycle. Validation of biosensor-like HepG2 spheroids by applying two genotoxic agents, benzo(a)pyrene and amino-1-methyl-6-phenylimidazo[4,5-b]pyridine with well-known mechanisms of action confirmed that sensing of fluorescent signals within the exposed cells corresponding to specific effects represents a powerful tool for the identification of (geno)toxic compounds. Thus, the resulting confocal imaging coupled with multiparametric flow cytometry in 3D hepatic spheroids represents an advanced biosensor-like approach that can provide more insight into the mechanism of action of genotoxic compounds due to the ability of simultaneous measurement of several effect related parameters and its applicability in toxicological studies as a high-content screening tool.

Declaration of competing interest

The authors declare that they have no known competing financial interests or personal relationships that could have appeared to influence the work reported in this paper.

Acknowledgment

The authors thank Klara Hercog, PhD for her technical assistance; Barbara Breznik, PhD (National Institute of Biology) for her valuable advice in confocal microscopy; and Miha Dominko, PhD (Institute for Economic Research) for his useful advice related to statistical methods and interpretations.

Appendix A. Supplementary data

Supplementary data to this article can be found online at <https://doi.org/10.1016/j.chemosphere.2021.132805>.

Funding sources

This work was supported by the Slovenian Research Agency [P1-0245, J1-2465 and MR-MŠtampar], and COST Action CA161119 (*In vitro* 3-D total cell guidance and fitness).

Associated content

The Supporting Information is available free of charge. List of used chemicals, figures showing the impact on the growth of spheroids and data for Comparative analysis of the compounds at different concentration levels (PDF).

Author contributions

The manuscript was written through the contributions of all authors. **Conceptualization:** Bojana Žegura, Martina Štampar; **Methodology:** Martina Štampar, Sonja Žabkar, Bojana Žegura; **Software:** Martina Štampar, Sonja Žabkar; **Validation:** Martina Štampar, Bojana Žegura, Sonja Žabkar; **Formal analysis:** Martina Štampar, Bojana Žegura, Sonja Žabkar; **Investigation:** Martina Štampar, Sonja Žabkar, Bojana Žegura; **Resources:** Metka Filipič, Bojana Žegura; **Data curation:** Martina Štampar, Bojana Žegura; **Writing – original draft:** Martina Štampar, Bojana Žegura; **Writing – review & editing:** Metka Filipič, Sonja Žabkar; **Visualization:** Martina Štampar, Sonja Žabkar, Bojana Žegura; **Supervision:** Bojana Žegura, Metka Filipič **Project administration:** Bojana Žegura, Metka Filipič **Funding acquisition:** Metka Filipič, Bojana Žegura.

Ethics approval

The authors declare no involving Human Participants and/or Animals. In the study human cell line was used, HepG2 cells (HB-8065™) obtained by the ATCC-Cell bank.

Consent to participate

Not applicable.

Consent for publication

Not applicable.

Availability of data and material

The authors confirm that the data supporting the findings of this study are available within the article [and/or] its supplementary materials. Generated raw data of this study are available from the corresponding author [BŽ] on request.

Code availability

Not applicable.

References

- Arlt, V.M., Stiborová, M., Henderson, C.J., Thiemann, M., Frei, E., Aimová, D., Singh, R., da Costa, G.G., Schmitz, O.J., Farmer, P.B., Wolf, C.R., Phillips, D.H., 2008. Metabolic activation of benzo[a]pyrene in vitro by hepatic cytochrome P450 contrasts with detoxification in vivo: experiments with hepatic cytochrome P450 reductase null mice. *Carcinogenesis* 29, 656–665. <https://doi.org/10.1093/carcin/bgn002>.
- Bande, O.J., Santillo, M.F., Ferguson, M., Wiesenfeld, P.L., 2012. In vitro toxicity screening of chemical mixtures using HepG2/C3A cells. *Food Chem. Toxicol.* 50, 1653–1659. <https://doi.org/10.1016/j.fct.2012.02.016>.
- Bartek, J., Lukas, J., 2001. Mammalian G1- and S-phase checkpoints in response to DNA damage. *Curr. Opin. Cell Biol.* [https://doi.org/10.1016/S0955-0674\(00\)00280-5](https://doi.org/10.1016/S0955-0674(00)00280-5).
- Bell, C.C., Hendriks, D.F.G., Moro, S.M.L., Ellis, E., Walsh, J., Renblom, A., Fredriksson Puigvert, L., Dankers, A.C.A., Jacobs, F., Snoeys, J., Sison-Young, R.L., Jenkins, R.E., Nordling, Å., Mkrtchian, S., Park, B.K., Kitteringham, N.R., Goldring, C.E.P., Lauschke, V.M., Ingelman-Sundberg, M., 2016. Characterization of primary human hepatocyte spheroids as a model system for drug-induced liver injury, liver function and disease. *Sci. Rep.* 6 <https://doi.org/10.1038/srep25187>.
- Bergant Loboda, K., Janežič, M., Štampar, M., Žegura, B., Filipič, M., Perdih, A., 2020. Substituted 4,5'-bithiazoles as catalytic inhibitors of human DNA topoisomerase II α . *J. Chem. Inf. Model.* 60, 3662–3678. <https://doi.org/10.1021/acs.jcim.0c00202>.

- Bokhari, M., Carnachan, R.J., Cameron, N.R., Przyborski, S.A., 2007. Culture of HepG2 liver cells on three dimensional polystyrene scaffolds enhances cell structure and function during toxicological challenge. *J. Anat.* 211, 567–576. <https://doi.org/10.1111/j.1469-7580.2007.00778.x>.
- Caino, M.C., Oliva, J.L., Jiang, H., Penning, T.M., Kazanietz, M.G., 2007. Benzo[a]pyrene-7,8-dihydrodiol promotes checkpoint activation and G 2/M arrest in human bronchoalveolar carcinoma H358 cells. *Mol. Pharmacol.* 71, 744–750. <https://doi.org/10.1124/mol.106.032078>.
- Coltman, N.J., Coke, B.A., Chatzi, K., Shepherd, E.L., Lalor, P.F., Schulz-Utermoehl, T., Hodges, N.J., 2021. Application of HepG2/C3A liver spheroids as a model system for genotoxicity studies. *Toxicol. Lett.* 345, 34–45. <https://doi.org/10.1016/j.toxlet.2021.04.004>.
- Conway, G.E., Shah, U.K., Llewellyn, S., Cervena, T., Evans, S.J., Al Ali, A.S., Jenkins, G. J., Clift, M.J.D., Doak, S.H., 2020. Adaptation of the in vitro micronucleus assay for genotoxicity testing using 3D liver models supporting longer-term exposure durations. *Mutagenesis* 35, 319–330. <https://doi.org/10.1093/mutage/geaa018>.
- Corvi, R., Madia, F., 2017. In vitro genotoxicity testing: Can the performance be enhanced?—NC-ND license. *Food Chem. Toxicol.* 106, 600–608. <https://doi.org/10.1016/j.fct.2016.08.024>. <http://creativecommons.org/licenses/by-nc-nd/4.0/>.
- Corvi, R., Madia, F., Worth, A., Whelan, M., 2013. EURL ECVAM Strategy to Avoid and Reduce Animal Use in Genotoxicity Testing. <https://doi.org/10.2788/43865>.
- den Braver-Sewradj, S.P., den Braver, M.W., Vermeulen, N.P.E., Commandeur, J.N.M., Richert, L., Vos, J.C., 2016. Inter-donor variability of phase I/phase II metabolism of three reference drugs in cryopreserved primary human hepatocytes in suspension and monolayer. *Toxicol. Vitro* 33, 71–79. <https://doi.org/10.1016/j.tiv.2016.02.013>.
- Edmondson, R., Broglie, J.J., Adcock, A.F., Yang, L., 2014. Three-dimensional cell culture systems and their applications in drug discovery and cell-based biosensors. *Assay Drug Dev. Technol.* 12, 207–218. <https://doi.org/10.1089/adt.2014.573>.
- Eilenberger, C., Rothbauer, M., Ehmoser, E.K., Ertl, P., Küpçü, S., 2019. Effect of spheroidal age on sorafenib diffusivity and toxicity in a 3D HepG2 spheroid model. *Sci. Rep.* 9. <https://doi.org/10.1038/s41598-019-41273-3>.
- Elje, E., Hesler, M., Rundén-Pran, E., Mann, P., Mariussen, E., Wagner, S., Dusinska, M., Kohl, Y., 2019. The comet assay applied to HepG2 liver spheroids. *Mutat. Res. Genet. Toxicol. Environ. Mutagen* 845, 403033. <https://doi.org/10.1016/j.mrgentox.2019.03.006>.
- Elje, E., Mariussen, E., Moriones, O.H., Bastús, N.G., Puentes, V., Kohl, Y., Dusinska, M., Rundén-Pran, E., 2020. Hepato(Geno)toxicity assessment of nanoparticles in a hepg2 liver spheroid model. *Nanomaterials* 10. <https://doi.org/10.3390/nano10030545>.
- Fey, S.J., Wrzesinski, K., 2012. Determination of drug toxicity using 3D spheroids constructed from an immortal human hepatocyte cell line. *Toxicol. Sci.* 127, 403–411. <https://doi.org/10.1093/toxsci/kfs122>.
- Fey, S.J., Korzeniowska, B., Wrzesinski, K., 2020. Response to and recovery from treatment in human liver-mimetic clinostat spheroids: a model for assessing repeated-dose drug toxicity. *Toxicol. Res. (Camb.)* 9, 379–389. <https://doi.org/10.1093/TOXRES/TFAA033>.
- Gomez-Lechon, M., Donato, M., Castell, J., Jover, R., 2004. Human hepatocytes in primary culture: the choice to investigate drug metabolism in man. *Curr. Drug Metabol.* 5, 443–462. <https://doi.org/10.2174/1389200043335414>.
- Guo, X., Seo, J., Li, X., Mei, N., 2019. Genetic toxicity assessment using liver cell models: past, present, and future. *00 J. Toxicol. Environ. Health Part B* 1–24. <https://doi.org/10.1080/10937404.2019.1692744>.
- Hamouchene, H., Arlt, V.M., Giddings, I., Phillips, D.H., 2011. Influence of cell cycle on responses of MCF-7 cells to benzo[a]pyrene. *BMC Genom.* 12, 333. <https://doi.org/10.1186/1471-2164-12-333>.
- Hercog, K., Maisanaba, S., Filipić, M., Sollner-Dolenc, M., Kač, L., Žegura, B., 2019. Genotoxic activity of bisphenol A and its analogues bisphenol S, bisphenol F and bisphenol AF and their mixtures in human hepatocellular carcinoma (HepG2) cells. *Sci. Total Environ.* 687, 267–276. <https://doi.org/10.1016/j.scitotenv.2019.05.486>.
- Hercog, K., Štampar, M., Stern, A., Filipić, M., Žegura, B., 2020. Application of advanced HepG2 3D cell model for studying genotoxic activity of cyanobacterial toxin cylindrospermopsin. *Environ. Pollut.* 265, 114965. <https://doi.org/10.1016/j.envpol.2020.114965>.
- Hockley, S.L., Arlt, V.M., Brewer, D., Giddings, I., Phillips, D.H., 2006. Time- and concentration-dependent changes in gene expression induced by benzo(a)pyrene in two human cell lines, MCF-7 and HepG2. *BMC Genom.* 7. <https://doi.org/10.1186/1471-2164-7-260>.
- Hs, F., M Š, Jm, V.-N., B, Ž., A, R.-W., 2021. Method to disassemble spheroids into core and rim for downstream applications such as flow cytometry, comet assay, transcriptomics, proteomics, and lipidomics. *Methods Mol. Biol.* 2273, 173–188. https://doi.org/10.1007/978-1-0716-1246-0_12.
- Hughes, B., 2008. Industry concern over EU hepatotoxicity guidance. *Nat. Rev. Drug Discov.* 7, 719. <https://doi.org/10.1038/nrd2677>.
- Hurrell, T., Lilley, K.S., Cromarty, A.D., 2019. Proteomic responses of HepG2 cell monolayers and 3D spheroids to selected hepatotoxins. *Toxicol. Lett.* 300, 40–50. <https://doi.org/10.1016/j.toxlet.2018.10.030>.
- Jeffy, B.D., Chen, E.J., Gudas, J.M., Romagnolo, D.F., 2000. Disruption of cell cycle kinetics by benzo[a]pyrene: inverse expression patterns of BRCA-1 and p53 in MCF-7 cells arrested in S and G2. *Neoplasia* 2, 460–470. <https://doi.org/10.1038/sj.neo.7900104>.
- Kastan, M.B., Lim, D.S., Kim, S.T., Xu, B., Canman, C., 2000. Multiple signaling pathways involving ATM. In: *Cold Spring Harbor Symposia on Quantitative Biology*. Cold Spring Harbor Laboratory Press, pp. 521–526. <https://doi.org/10.1101/sqb.2000.65.521>.
- Kirkland, D., Aardema, M., Henderson, L., Müller, L., 2005. Erratum: evaluation of the ability of a battery of three in vitro genotoxicity tests to discriminate rodent carcinogens and non-carcinogens I. Sensitivity, specificity and relative predictivity (Mutation Research - genetic Toxicology and Environmental Mut. Mutat. Res. Genet. Toxicol. Environ. Mutagen 588, 70. <https://doi.org/10.1016/j.mrgentox.2005.10.002>).
- Kirkland, D., Pfühler, S., Tweats, D., Aardema, M., Corvi, R., Darroudi, F., Elhajouji, A., Glatt, H., Hastwell, P., Hayashi, M., Kasper, P., Kirchner, S., Lynch, A., Marzin, D., Maurici, D., Meunier, J.-R., Müller, L., Nohynek, G., Parry, J., Parry, E., Thybaud, V., Tice, R., van Benthem, J., Vanparys, P., White, P., 2007. How to reduce false positive results when undertaking in vitro genotoxicity testing and thus avoid unnecessary follow-up animal tests: report of an ECVAM Workshop. *Mutat. Res. Toxicol. Environ. Mutagen.* 628, 31–55. <https://doi.org/10.1016/J.MRGENTOX.2006.11.008>.
- Knasmüller, S., Mersch-Sundermann, V., Kevekordes, S., Darroudi, F., Huber, W.W., Hoelzl, C., Bichler, J., Majer, B.J., 2004. Use of human-derived liver cell lines for the detection of environmental and dietary genotoxicants; Current state of knowledge. In: *Toxicology*. Elsevier, pp. 315–328. <https://doi.org/10.1016/j.tox.2004.02.008>.
- Kopp, B., Vignard, J., Mirey, G., Fessard, V., Zalko, D., Le Hégarat, L., Audebert, M., 2018. Genotoxicity and mutagenicity assessment of food contaminant mixtures present in the French diet. *Environ. Mol. Mutagen.* 59, 742–754. <https://doi.org/10.1002/em.22214>.
- LeCluyse, E.L., 2001. Human hepatocyte culture systems for the in vitro evaluation of cytochrome P450 expression and regulation. *Eur. J. Pharmaceut. Sci.* 13, 343–368. [https://doi.org/10.1016/S0928-0987\(01\)00135-X](https://doi.org/10.1016/S0928-0987(01)00135-X).
- Llewellyn, S.V., Conway, G.E., Shah, U.K., Evans, S.J., Jenkins, G.J.S., Clift, M.J.D., Doak, S.H., 2020. Advanced 3D liver models for in vitro genotoxicity testing following long-term nanomaterial exposure. *JoVE* 2020, 1–10. <https://doi.org/10.3791/61141>.
- Lodish, H., Berk, A., Zipursky, S.L., Matsudaira, P., Baltimore, D., Darnell, J., 2000. *DNA Damage and Repair and Their Role in Carcinogenesis*.
- Löffler, H., Bochtler, T., Fritz, B., Tews, B., Ho, A.D., Lukas, J., Bartek, J., Krämer, A., 2007. DNA damage-induced accumulation of centrosomal Chk1 contributes to its checkpoint function. *Cell Cycle* 6, 2541–2548. <https://doi.org/10.1016/j.cc.6.20.4810>.
- Mahadevan, B., Snyder, R.D., Waters, M.D., Benz, R.D., Kemper, R.A., Tice, R.R., Richard, A.M., 2011. Genetic toxicology in the 21st century: reflections and future directions. *Environ. Mol. Mutagen.* <https://doi.org/10.1002/em.20653>.
- Mandon, M., Huet, S., Dubreil, E., Fessard, V., Le Hégarat, L., 2019. Three-dimensional HepaRG spheroids as a liver model to study human genotoxicity in vitro with the single cell gel electrophoresis assay. *Sci. Rep.* 9. <https://doi.org/10.1038/s41598-019-47114-7>.
- Murray, Andrew, Tim Hunt, W.H., 1994. The cell cycle: an introduction. *Mol. Reprod. Dev.* 39, 247. <https://doi.org/10.1002/mrd.1080390223>.
- Patra, B., Peng, C.-C., Liao, W.-H., Lee, C.-H., Tung, Y.-C., 2016. Drug testing and flow cytometry analysis on a large number of uniform sized tumor spheroids using a microfluidic device. *Sci. Rep.* 6, 1–12. <https://doi.org/10.1038/srep21061>.
- Pezdiric, M., Žegura, B., Filipić, M., 2013. Genotoxicity and induction of DNA damage responsive genes by food-borne heterocyclic aromatic amines in human hepatoma HepG2 cells. *Food Chem. Toxicol.* 59, 386–394. <https://doi.org/10.1016/j.fct.2013.06.030>.
- Pfühler, S., van Benthem, J., Curren, R., Doak, S.H., Dusinska, M., Hayashi, M., Heflich, R.H., Kidd, D., Kirkland, D., Luan, Y., Ouedraogo, G., Reisinger, K., Sofuni, T., van Acker, F., Yang, Y., Corvi, R., 2020. Use of in vitro 3D tissue models in genotoxicity testing: strategic fit, validation status and way forward. Report of the working group from the 7th International Workshop on Genotoxicity Testing (IWGT). *Mutat. Res. Genet. Toxicol. Environ. Mutagen.* <https://doi.org/10.1016/j.mrgentox.2020.503135>.
- Pinhoiro, J., Bates, D., DebRoy, S., Sarkar, D., 2007. *R Development Core Team*. 2010. *Nlme: Linear and Nonlinear Mixed Effects Models. R Package, version 3*.
- Ramaiahgari, S.C., Den Braver, M.W., Herpers, B., Terpstra, V., Commandeur, J.N.M., Van De Water, B., Price, L.S., 2014. A 3D in vitro model of differentiated HepG2 cell spheroids with improved liver-like properties for repeated dose high-throughput toxicity studies. *Arch. Toxicol.* 88, 1083–1095. <https://doi.org/10.1007/s00204-014-1215-9>.
- Scholzen, T., Gerdes, J., 2000. The Ki-67 protein: from the known and the unknown. *J. Cell. Physiol.* [https://doi.org/10.1002/\(SICI\)1097-4652\(200003\)182:3<311::AID-JCP1>3.0.CO;2;9](https://doi.org/10.1002/(SICI)1097-4652(200003)182:3<311::AID-JCP1>3.0.CO;2;9).
- Shah, U.K., Mallia, J. de O., Singh, N., Chapman, K.E., Doak, S.H., Jenkins, G.J.S., 2018. A three-dimensional in vitro HepG2 cells liver spheroid model for genotoxicity studies. *Mutat. Res. Genet. Toxicol. Environ. Mutagen* 825, 51–58. <https://doi.org/10.1016/j.mrgentox.2017.12.005>.
- Shah, U.-K., Verma, J.R., Chapman, K.E., Wilde, E.C., Tonkin, J.A., Brown, M.R., Johnson, G.E., Doak, S.H., Jenkins, G.J., 2020. OUP accepted manuscript. *Mutagenesis* 1–8. <https://doi.org/10.1093/mutage/geaa029>.
- Štampar, M., Tomc, J., Filipić, M., Žegura, B., 2019. Development of in vitro 3D cell model from hepatocellular carcinoma (HepG2) cell line and its application for genotoxicity testing. *Arch. Toxicol.* 93, 3321–3333. <https://doi.org/10.1007/s00204-019-02576-6>.
- Štampar, M., Breznik, B., Filipić, M., Žegura, B., 2020a. Characterization of in vitro 3D cell model developed from human hepatocellular carcinoma (HepG2) cell line. *Cells* 9, 2557. <https://doi.org/10.3390/cells9122557>.
- Štampar, M., Frandsen, H.S., Rogowska-Wrzesinska, A., Wrzesinski, K., Filipić, M., Žegura, B., 2020b. Hepatocellular carcinoma (HepG2/C3A) cell-based 3D model for genotoxicity testing of chemicals. *Sci. Total Environ.*, 143255. <https://doi.org/10.1016/j.scitotenv.2020.143255>.
- Stellas, D., Souliotis, V.L., Bekyrou, M., Smirlis, D., Kirsch-Volders, M., Degraasi, F., Cundari, E., Kyrtopoulos, S.A., 2014. Benzo[a]pyrene-induced cell cycle arrest in HepG2 cells is associated with delayed induction of mitotic instability. *Mutat. Res.*

- Fund Mol. Mech. Mutagen 769, 59–68. <https://doi.org/10.1016/j.mrfmmm.2014.07.004>.
- Waldherr, M., Lundt, N., Klaas, M., Betzold, S., Wurdack, M., Baumann, V., Estrecho, E., Nalitov, A., Cherotchenko, E., Cai, H., Ostrovskaya, E.A., Kavokin, A.V., Tongay, S., Klemmt, S., Höfling, S., Schneider, C., 2018. Observation of bosonic condensation in a hybrid monolayer MoSe₂-GaAs microcavity. Nat. Commun. 9 <https://doi.org/10.1038/s41467-018-05532-7>.
- Wilsker, D., Petermann, E., Helleday, T., Bunz, F., 2008. Essential function of Chk1 can be uncoupled from DNA damage checkpoint and replication control. Proc. Natl. Acad. Sci. U.S.A. 105, 20752–20757. <https://doi.org/10.1073/pnas.0806917106>.
- Wrzesinski, K., Fey, S.J., 2013. After trypsinisation, 3D spheroids of C3A hepatocytes need 18 days to re-establish similar levels of key physiological functions to those seen in the liver. Toxicol. Res. (Camb). 2, 123–135. <https://doi.org/10.1039/c2tx20060k>.
- Wrzesinski, K., Fey, S.J., 2015. From 2D to 3D - a new dimension for modelling the effect of natural products on human tissue. Curr. Pharmaceut. Des. 21, 5605–5616. <https://doi.org/10.2174/1381612821666151002114227>.
- Wrzesinski, K., Rogowska-Wrzesinska, A., Kanlaya, R., Borkowski, K., Schwämmle, V., Dai, J., Joensen, K.E., Wojdyla, K., Carvalho, V.B., Fey, S.J., 2014. The cultural divide: exponential growth in classical 2D and metabolic equilibrium in 3D environments. PLoS One 9. <https://doi.org/10.1371/journal.pone.0106973>.
- Wrzesinski, K., Alnøe, S., Jochumsen, H.H., Mikkelsen, K., Bryld, T.D., Vistisen, J.S., Alnøe, P.W., Fey, S.J., 2021. A purpose-built system for culturing cells as *in vivo*-mimetic 3D structures. Biomech. Funct. Tissue Eng. <https://doi.org/10.5772/INTECHOPEN.96091> [Working Title].
- Zhu, H., Boobis, A.R., Gooderham, N.J., 2000. The food-derived carcinogen 2-amino-1-methyl-6-phenylimidazo[4,5-b]pyridine activates S-phase checkpoint and apoptosis, and induces gene mutation in human lymphoblastoid TK6 cells. Cancer Res. 60, 1283–1289.